AGU PUBLICATIONS

Geophysical Research Letters

RESEARCH LETTER
10.1002/2014GL062390

Key Points:
- Small Fe/Na flux ratio indicates cosmic dust enters atmosphere at slow velocity
- The majority of the mass influx originates from the Jupiter Family of Comets
- The total cosmic dust influx is estimated to be 150 ± 38 t/d

Correspondence to:
X. Chu,
Xinzhao.Chu@colorado.edu

Citation:
Huang, W., X. Chu, C. S. Gardner, J. D. Carrillo-Sánchez, W. Feng, J. M. C. Plane, and D. Nesvorný (2015), Measurements of the vertical fluxes of atomic Fe and Na at the mesopause: Implications for the velocity of cosmic dust entering the atmosphere, *Geophys. Res. Lett.*, *42*, 169–175, doi:10.1002/2014GL062390.

Received 31 OCT 2014
Accepted 17 DEC 2014
Accepted article online 19 DEC 2014
Published online 8 JAN 2015

Measurements of the vertical fluxes of atomic Fe and Na at the mesopause: Implications for the velocity of cosmic dust entering the atmosphere

Wentao Huang[1], Xinzhao Chu[1,2], Chester S. Gardner[3], Juan D. Carrillo-Sánchez[4], Wuhu Feng[4], John M. C. Plane[4], and David Nesvorný[5]

[1]Cooperative Institute for Research in Environmental Sciences, University of Colorado Boulder, Boulder, Colorado, USA, [2]Department of Aerospace Engineering Sciences, University of Colorado Boulder, Boulder, Colorado, USA, [3]Department of Electrical and Computer Engineering, University of Illinois at Urbana-Champaign, Urbana, Illinois, USA, [4]School of Chemistry, University of Leeds, Leeds, UK, [5]Department of Space Studies, Southwest Research Institute, Boulder, Colorado, USA

Abstract The downward fluxes of Fe and Na, measured near the mesopause with the University of Colorado lidars near Boulder, and a chemical ablation model developed at the University of Leeds, are used to constrain the velocity/mass distribution of the meteoroids entering the atmosphere and to derive an improved estimate for the global influx of cosmic dust. We find that the particles responsible for injecting a large fraction of the ablated material into the Earth's upper atmosphere enter at relatively slow speeds and originate primarily from the Jupiter Family of Comets. The global mean Na influx is 17,200 ± 2800 atoms/cm^2/s, which equals 298 ± 47 kg/d for the global input of Na vapor and 150 ± 38 t/d for the global influx of cosmic dust. The global mean Fe influx is 102,000 ± 18,000 atoms/cm^2/s, which equals 4.29 ± 0.75 t/d for the global input of Fe vapor.

1. Introduction

The mesospheric metal layers are formed by the ablation of high-speed cosmic dust particles when they are heated to high temperatures caused by friction with the Earth's upper atmosphere. The metal atoms are injected into the lower thermosphere and upper mesosphere (80–120 km altitude) [*Vondrak et al.*, 2008; *Janches et al.*, 2009] and are then transported downward to chemical sinks below about 85 km by advection, eddy diffusion, and wave effects. The densities and vertical fluxes of mesospheric metals like Fe and Na are closely related to their meteoric influxes, their chemistries, and to the speed with which they are transported downward [e.g., *Plane*, 2004; *Gardner and Liu*, 2010; *Marsh et al.*, 2013a; *Feng et al.*, 2013]. In fact, the meteoric influxes of Fe and Na can be determined by measuring the vertical fluxes of these species at altitudes below where they are injected into the atmosphere, but above their chemical sinks, where the majority of the Fe and Na are still in atomic form [*Gardner et al.*, 2014]. Thus, knowledge of the Fe and Na fluxes provides important insights on the influx of all meteoric species and on the transport of gaseous constituents in the mesopause region.

The vertical flux of mesospheric Na has been measured with high-resolution, zenith pointing Doppler lidars at several locations in both the Northern and Southern Hemispheres, and the results have been used to estimate the global influx of cosmic dust [*Gardner et al.*, 2014]. During August and September 2010, an Fe Boltzmann temperature lidar and a Na Doppler lidar were operated simultaneously at the Table Mountain Lidar Facility (40.13°N, 105.24°W) north of Boulder, Colorado, and used to observe a common volume of the mesopause region [*Huang et al.*, 2013]. We use this unique data set to derive the vertical fluxes of both Fe and Na at this site. We are particularly interested in the measured ratio of the Fe and Na fluxes because this ratio is especially sensitive to the velocity/mass distribution of the cosmic dust particles.

Meteor velocities range from a low value of 11.2 km/s for particles in the same orbit as Earth (prograde orbit) to 72.5 km/s for particles in a retrograde orbit [*Baggaley*, 2002]. If the velocities of the majority of the particles are fast, then these particles will completely vaporize at high altitudes and the ratio of the Fe flux to the Na flux will be equal to the ratio of their elemental abundances in the dust particles (~15). However, if the

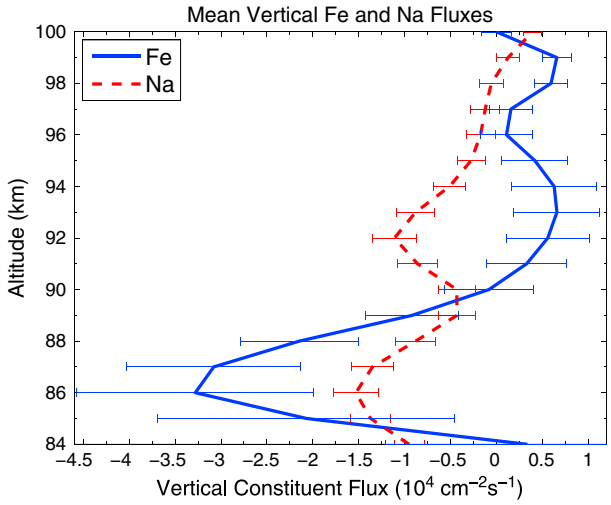

Figure 1. Profiles of the mean vertical fluxes of atomic Fe (blue solid line) and Na (red dashed line) measured at the Table Mountain Lidar Facility in August–September 2010.

particle velocities are slow, then many of the more massive particles will only partially ablate. In this case a greater fraction of the more volatile Na atoms will evaporate from the particles compared to the less volatile Fe, so that the flux ratio will be less than the ratio of their elemental abundances. In this paper, we use the measured flux ratio at Table Mountain and the Chemical Ablation Model (CABMOD) developed at the University of Leeds [*Vondrak et al.*, 2008] to constrain the velocity/mass distribution of the dust particles and derive an improved estimate for the global influx of cosmic dust.

2. Observations

Observations of vertical wind, temperature, Fe density, and Na density profiles between 80 and 110 km were made during 12 nights (59 h in total) in August and September 2010 with an Fe Boltzmann temperature lidar and a Na Doppler lidar at Table Mountain. In sections 3 and 4 of their paper, *Huang et al.* [2013] provide detailed descriptions of the lidar specifications and measurement capabilities, the observational scenarios, and the data processing for this unique data set. The vertical constituent flux is defined as the expected value of the product of the vertical wind and the constituent density. The vertical winds measured by the Na Doppler lidar were combined with the Fe and Na densities measured by both instruments to derive the vertical fluxes of Fe and Na using the standard data analysis techniques [e.g., *Gardner and Liu*, 2010]. Because the wind and densities were derived with a vertical resolution of 960 m and a temporal resolution of 10 min, the data include the transport effects of most gravity waves but exclude the effects of turbulence and vertical advection. Hence, the directly measured fluxes do not include the advective fluxes, which are negligible [*Gardner et al.*, 2014], nor do they include the important eddy flux contributions.

The Fe and Na eddy fluxes were determined by using the well-known relationship between the eddy flux and the eddy diffusivity (k_{zz})

$$\begin{aligned}\overline{w\rho_{\mathrm{Na}}}|_{\mathrm{Eddy}} &= -k_{zz}\left(\frac{1}{H}+\frac{1}{\overline{T}}\frac{\partial\overline{T}}{\partial z}+\frac{1}{\overline{\rho}_{\mathrm{Na}}}\frac{\partial\overline{\rho}_{\mathrm{Na}}}{\partial z}\right)\overline{\rho}_{\mathrm{Na}}\\ \overline{w\rho_{\mathrm{Fe}}}|_{\mathrm{Eddy}} &= -k_{zz}\left(\frac{1}{H}+\frac{1}{\overline{T}}\frac{\partial\overline{T}}{\partial z}+\frac{1}{\overline{\rho}_{\mathrm{Fe}}}\frac{\partial\overline{\rho}_{\mathrm{Fe}}}{\partial z}\right)\overline{\rho}_{\mathrm{Fe}}\end{aligned}, \quad (1)$$

where H is the pressure scale height, $\overline{T}$ is the mean temperature profile, and $\overline{\rho}_{\mathrm{Na}}$ and $\overline{\rho}_{\mathrm{Fe}}$ are the mean Na and Fe density profiles and the overbar denotes sample average. The Fe and Na eddy flux profiles were computed using equation (1) and a fixed value of 42 m^2/s for k_{zz}, which is the zonal mean value at about 86 km for August and September at 40°N predicted by the gravity wave parameterization module in the Whole Atmosphere Community Climate Model (WACCM) [*Marsh et al.*, 2013b]. We assumed an uncertainty of ±30% for k_{zz} [*Gardner et al.*, 2014]. The sums of the gravity wave- and turbulence-induced flux profiles for Fe and Na are plotted in Figure 1. Both profiles reach their maximum values at 86 km. The corresponding Fe and Na density profiles are plotted in Figure 2.

Summarized in Table 1 are the observed fluxes and atomic densities of Fe and Na at 86 km. This altitude is below the peaks of both layers in the region where chemical processes are beginning to produce Fe and Na compounds, which the lidars cannot observe. For this time of year and latitude, the WACCM Fe and Na models [*Feng et al.*, 2013; *Marsh et al.*, 2013a] predict that 77.5% of the Fe and 93.0% of the Na are in atomic form at 86 km. Because Na and Fe are minor species, the fraction of

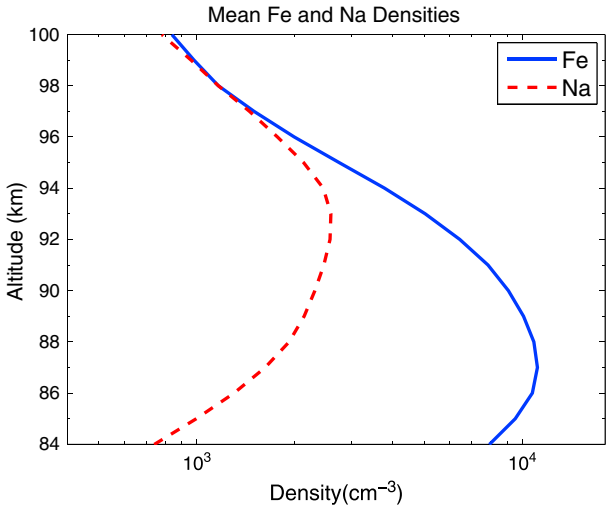

Figure 2. Profiles of the mean densities of atomic Fe and Na measured at the Table Mountain Lidar Facility in August–September 2010.

these metals in atomic form is primarily a function of the chemical model used in WACCM and does not depend on the magnitude of their influxes or injection profiles. In fact, other models of the mesospheric metals, which were developed using much larger meteoric influx values than WACCM [e.g., *Plane*, 2004], also show that the majority of Na and Fe between 85 and 90 km are in atomic form. Therefore, to account for the vertical transport of the Fe and Na compounds, the observed atomic fluxes are scaled by the inverse of these atomic fractions to yield the total species fluxes, which are equal to the meteoric influxes of these species above 86 km [*Gardner et al.*, 2014]. The ratio of the total Fe flux to the total Na flux is given by

$$\frac{\text{Total Fe Species Flux at 86 km}}{\text{Total Na Species Flux at 86 km}} = \frac{\text{Observed Atomic Fe Flux at 86 km}}{\text{Observed Atomic Na Flux at 86 km}} \cdot \frac{0.930}{0.775} = 2.57 \pm 1.09\,. \tag{2}$$

The composition of the primitive CI carbonaceous chondrite meteorites is believed to be the most representative of the original solar nebula and is therefore an accepted reference for the composition of the cosmic dust particles [*Jessberger et al.*, 2001]. *Lodders et al.* [2009] compiled numerous analyses of the Orgueil meteorite as the standard CI rock, because it is the most massive of the CI-chondrite falls and therefore it is the one that has been analyzed the most. They report a mean composition by mass of 185,000 ± 5550 ppm for Fe and 4990 ± 250 ppm for Na. Hence, the ratio of the elemental abundances of Fe and Na in CI chondrites is [Fe]/[Na] = 15.26 ± 0.89.

The meteoric influxes of Fe and Na above 86 km altitude are equal to the total number of atoms of the species in the dust particles, times the fraction of the species ablated from all the dust particles, times the fraction ablated above 86 km. The ratio of the meteoric influx of Fe atoms to the influx of Na atoms is given by

$$\frac{\text{Meteoric Influx of Fe Atoms Above 86 km}}{\text{Meteoric Influx of Na Atoms Above 86 km}} = (15.26 \pm 0.89) \cdot \frac{\text{Fraction of Fe Atoms Ablated}}{\text{Fraction of Na Atoms Ablated}} \cdot \frac{\text{Fraction of Fe Ablated Above 86 km}}{\text{Fraction of Na Ablated Above 86 km}}\,. \tag{3}$$

The particles entering the atmosphere at high velocities, greater than about 30 km/s, will be completely vaporized at high altitudes in the lower thermosphere and upper mesosphere above 86 km [*Vondrak et al.*, 2008; *Janches et al.*, 2009], and so the ratio of the meteoric influxes of Fe and Na will be close to 15. The fact that the flux ratio measured by the lidars, 2.57 ± 1.09, is much less than 15.26 ± 0.89 is compelling evidence that the mean particle velocity is considerably less than 30 km/s.

Table 1. Characteristics of Fe and Na Observed at the Table Mountain Lidar Facility, Colorado, at 86 km

Parameter	Fe	Na
Gravity wave + eddy flux	$-32{,}800 \pm 12{,}900$ cm^{-2} s^{-1}	$-15{,}300 \pm 2{,}400$ cm^{-2} s^{-1}
Mean atomic density	10,750 cm^{-3}	1,300 cm^{-3}
Effective vertical transport velocity	-3.1 cm s^{-1}	-11.8 cm s^{-1}
WACCM atomic fraction	0.775	0.930
Total species flux	$-42{,}320 \pm 16{,}600$ cm^{-2} s^{-1}	$-16{,}450 \pm 2{,}600$ cm^{-2} s^{-1}

Table 2. Characteristics of Particle Velocity/Mass Distribution Models

Particle Model	HPLA Radar[a]	LDEF[b]	Zodiacal Cloud[c]
Mean particle velocity	~30 km s^{-1}	~18 km s^{-1}	~14.5 km s^{-1}
Total fraction of Fe ablated	0.9670	0.5550	0.1551
Fraction of Fe ablated above 86 km	0.9989	0.6086	0.5200
Total fraction of Na ablated	0.9912	0.8217	0.3980
Fraction of Na ablated above 86 km	1.0000	0.9770	0.9780
$\frac{\text{Meteoric Influx of Fe Atoms Above 86 km}}{\text{Meteoric Influx of Na Atoms Above 86 km}}$	14.87 ± 0.87	6.42 ± 0.37	3.16 ± 0.18

[a] *Fentzke and Janches* [2008] and *Janches et al*. [2014].
[b] *McBride et al*. [1999].
[c] *Nesvorný et al*. [2010, 2011].

3. Cosmic Dust Velocity/Mass Distribution Models

Several groups, employing a variety of observational data, have proposed different models for the particle velocity/mass distribution. In this paper, we focus on three of those models. The dominant contribution to the influx of cosmic dust comes from the sporadic meteor background, not from meteor showers. These submillimeter particles weigh between 10^{-11} and 10^{-4} g [*Plane*, 2012]. Janches and coworkers employed the Arecibo incoherent scatter radar in high-power large-aperture (HPLA) meteor mode for observations of meteor head echoes to develop a particle velocity distribution that has a mean velocity of about 30 km/s [*Fentzke and Janches*, 2008; *Janches et al*., 2008, 2014; *Pifko et al*., 2013]. This model incorporates the six known meteoroid radiant sources, as observed by the radars [*Janches et al*., 2006], so that the particle influx is modeled as a function of time of day, season, geographic location, and entry angle. Because the radar observations are known to be biased toward the faster particles, which create sufficient ionization to generate a detectable radar reflection [*Pifko et al*., 2013], recent work has focused on confirming that the HPLA radar at the Arecibo Observatory is able to observe the slower particles with velocities between 11.2 and 20 km/s [*Janches et al*., 2014].

Love and Brownlee [1993] analyzed the size distribution of meteoroids by measuring the hypervelocity impact craters found on the space-facing end of the Long Duration Exposure Facility (LDEF) satellite. They chose a mean particle velocity of 16.9 km/s to derive the particle mass distribution from the crater size measurements. *McBride et al*. [1999] used the LDEF data and meteor radar observations to develop a more realistic velocity/mass distribution with a mean velocity of ~18 km/s. *Nesvorný et al*. [2010, 2011] employed zodiacal cloud observations and model calculations to derive the velocity/mass distribution for Jupiter Family Cometary particles, which are believed to constitute more than 70% of the particle mass accreted by the Earth. The velocity model developed by Nesvorný and coworkers for these particles peaks near 12 km/s, and the mean value is approximately 14.5 km/s.

Vaporization of cosmic dust in the atmosphere involves several processes that depend on the mass and velocity of the particles as well as the volatility of their constituents. These include sputtering caused by inelastic collisions with air molecules before the particle melts, diffusion of volatile constituents through the molten particle, followed by evaporation of atoms and oxides from the melt. *Vondrak et al*. [2008] developed CABMOD to characterize the ablation of the more abundant elements as a function of altitude, taking into account the mass and velocity of the dust particles. They find that volatile constituents like Na and K evaporate rapidly at the highest altitudes, as soon as the particle melts, followed by the main constituents Si, Fe, and Mg, a few kilometers lower, when the particle temperature reaches ~1850 K. Because CABMOD calculates the injection profiles for the particle constituents as a function of the particle size, velocity, and entry angle, it can be used to predict the flux ratio needed in equation (3) once the velocity/mass distribution is specified.

CABMOD was used to compute the total Fe to Na flux ratio, for the velocity/mass distribution models proposed by Janches and coworkers based on radar observations, by Nesvorný and coworkers based on zodiacal light measurements, and by *Love and Brownlee* [1993] and *Mcbride et al*. [1999] to interpret the meteoroid impact data from the LDEF satellite. The CABMOD computations employed an improved Monte Carlo procedure for sampling the particle mass/velocity distribution, which yields slightly different results for the ablation statistics than were reported in the original *Vondrak et al*. [2008] paper. The results are tabulated in Table 2. For the fast radar model, where almost all of the Fe and Na vaporize, the calculated flux ratio (14.87 ± 0.87) is

nearly equal to the ratio of the elemental abundances of Fe and Na in CI chondrites. For the slower LDEF model, the ratio is much smaller (6.42 ± 0.37), because more of the Na is ablated compared to the less volatile Fe. Furthermore, the Na is injected at higher altitudes than Fe. For the slowest zodiacal cloud model, comprised entirely of Jupiter Family Cometary particles, the flux ratio is smallest (3.16 ± 0.18) and approximately equal to the flux ratio measured by the Table Mountain lidars (2.57 ± 1.09). In fact, the small difference between the flux ratio predicted by CABMOD and the zodiacal cloud model and the ratio measured by the lidars, 0.59 ± 1.1, is not statistically significant from zero. This result is direct and compelling evidence that the particles responsible for injecting a large fraction of the ablated material into the Earth's upper atmosphere enter at relatively slow speeds because they are traveling in prograde orbits around the Sun and originate primarily from the Jupiter Family of Comets, as modeled by *Nesvorný et al*. [2010, 2011].

4. Discussion

The effective vertical transport velocity of a constituent is defined as its vertical flux divided by its density. For the Table Mountain data we find that the vertical transport velocity at 86 km is −3 cm/s for Fe and −12 cm/s for Na. While the speed of the dynamical transport of these species by dissipating gravity waves, tides, and planetary waves is identical, the speeds of chemical and eddy transport differ because they depend on the chemistries and concentration profiles of the species [*Gardner and Liu*, 2010]. The effective lifetime of the atomic species in the metal layer is defined as the layer abundance divided by the total meteoric influx. The mean abundances are 10.65×10^9 cm^{-2} and 3.45×10^9 cm^{-2}, respectively, for Fe and Na at Table Mountain for August–September 2010 [*Huang et al*., 2013]. The ratio of the Fe to Na column abundance equals 3.1, which is consistent with the measured flux ratio and also implies that the particle velocities must be slow. The total meteoric influxes of Fe and Na vapor can be estimated by dividing the total species fluxes at 86 km listed in Table 1 by the fraction of the species ablated above 86 km for the zodiacal cloud model (see Table 2). We find that the Fe lifetime is ~36 h and the Na lifetime is ~57 h. For this time of year the meridional winds average about −20 m/s between 85 and 90 km [*Gardner and Liu*, 2007], so that once an Fe atom is ablated it could be transported as far as 2600 km southward before it is consumed by chemistry. A Na atom could be transported as far as 4000 km. Hence, the Fe and Na atoms observed above Table Mountain were injected into the atmosphere as far away as several thousand kilometers and then advected by the upper atmosphere winds to the site.

Recently, *Gardner et al*. [2014] used Na flux observations (at 87.5 km) made throughout the year at the Starfire Optical Range, New Mexico (SOR, 35.0°N, 106.5°W), to estimate the daily mean global influxes of Na vapor and cosmic dust. These researchers used the original CABMOD calculations of the Na ablation fractions for the LDEF velocity/mass model to estimate the total Na vapor and cosmic dust influxes at SOR. They then used WACCM predictions of the global distribution of vertical transport processes to scale the SOR observations to obtain the global means. By using the more accurate zodiacal cloud velocity/mass model evaluated here (Note that the fraction of Na ablated above 87.5 km for the zodiacal cloud model is 0.833.) and the SOR observations, we find that the global mean Na influx is $17{,}200 \pm 2800$ atoms/cm^2/s, which corresponds to 298 ± 47 kg/d for the global input of Na vapor and 150 ± 38 t/d for the global influx of cosmic dust. To estimate the uncertainties, we used the approach of *Gardner et al*. [2014]. Although this new estimate for the total cosmic dust influx is larger by more than a factor of 2, the amount of Na that is vaporized is only 7% larger, because the zodiacal cloud particle velocities are slower than the LDEF velocity model so a smaller fraction of the mass vaporizes. A significant fraction of the total influx falls to Earth as cosmic spherules (melted) and unmelted meteorites. The global mean Fe influx is $102{,}000 \pm 18{,}000$ atoms/cm^2/s, which equals 4.29 ± 0.75 t/d for the global input of Fe vapor. Notice that according to equation (3), the ratio of the total meteoric influxes of Fe and Na (~6) is simply equal to the ratio of their elemental abundances (15.26) in the dust particles times the ratio of their total ablation fractions (0.39).

Estimates of the global cosmic dust influx derived by other workers range from 0.4 to 110 t/d. Our updated estimate of 150 ± 38 t/d is at the high end of this range, where it is in good accord with estimates based upon the accumulation rates of cosmic elements in polar ice cores and deep-sea sediments and derived spaceborne dust detection (see *Plane* [2012] for summary). In fact, *Love and Brownlee* [1993] deduced the value of 110 ± 55 t/d from measurements of the LDEF crater size data by inferring the particle kinetic energy

and mass distributions assuming a particle velocity of 16.9 km/s. The mean particle velocity of the zodiacal cloud model is 14.5 km/s. If the LDEF crater data are reinterpreted using this slower velocity, the total mass influx scales by the square of the velocity ratio, $(16.9/14.5)^2 = 1.358$, because the kinetic energy is proportional to the particle mass times the square of the impact velocity. In this case, the LDEF data set predicts a value of 149 ± 75 t/d for the total mass influx, which is nearly identical to the updated value derived from the SOR Na flux observations and the CABMOD calculations. Our estimate is significantly larger than the value of 5 ± 2 t/d derived by *Mathews et al.* [2001] from Arecibo radar observations and the 0.4–5 t/d derived by modeling the mesospheric Na, Fe, and Mg layers [*Marsh et al.*, 2013a; *Feng et al.*, 2013; *Langowski et al.*, 2014]. It is also larger than the value of 41 t/d derived by *Nesvorný et al.* [2011] from their zodiacal cloud model.

Our results were derived by employing a zodiacal cloud model composed entirely of Jupiter Family Cometary (JFC) particles. *Nesvorný et al.* [2011] suggest that the dust contribution from collisions between asteroids could be as much as 30%. These particles enter the Earth's atmosphere with velocities that are slower than the JFC particles [*Nesvorný et al.*, 2010]. Consequently, a smaller fraction of the asteroidal particle mass ablates compared to the JFC particles, the ablation occurs at lower altitudes and less Fe compared to Na ablates from the asteroidal particles. The overall impact of the asteroidal particles is to reduce the Fe:Na flux ratio predicted by equation (3) and to increase the predicted total mass influx of cosmic dust. In fact, if more accurate, longer-term Na and Fe flux observations can be acquired, it may be possible to use the measured flux ratio to determine what fraction of the total particle mass originates from the asteroid belt. Similarly, the meteors observed by the HPLA radars represent a different family of very fast particles that may originate from outside the solar system. Inclusion of these particles in the velocity/mass model would increase the predicted Fe:Na flux ratio and decrease the total mass influx. Estimates suggest that these fast particles represent at most ~3.5% (5 ± 2 t/d) [*Mathews et al.*, 2001] of the total influx.

Because the particle velocities for the zodiacal cloud model are relatively slow, a smaller fraction of the particle mass ablates and this has important implications for numerous atmospheric processes [*Plane*, 2012]. For example, the ablated atoms and the meteoric smoke particles (MSPs), which they form, are involved in a broad array of chemical processes, play important roles in the formation of mesospheric and stratospheric clouds, and, when the iron-rich MSPs settle into the Southern Ocean around Antarctica [*Dhomse et al.*, 2013], they fertilize the growth of phytoplankton, which impacts the atmospheric CO_2 cycle. Consequently, it is the influx of ablated material, not the total mass, that needs to be reconciled with atmospheric modeling of the mesospheric metal layers, measurements of meteoric smoke, measurements of cosmic elements in ice cores and sea bed sediments, and as we have done here, with measurements of the atmospheric fluxes of mesospheric Fe and Na.

Acknowledgments

We sincerely acknowledge Zhangjun Wang, Weichun Fong, and John A. Smith for their contributions to the lidar measurements at Table Mountain. This analysis and the lidar work were supported in part by National Science Foundation grants AGS 1115224, AGS 1115725, AGS 1136272, ANT 0839091, PLR 1246405, and PLR 1246431. The CABMOD modeling work was supported by the European Research Council (project 291332-CODITA). The data and programs used in this work are available upon request.

The Editor thanks two anonymous reviewers for their assistance in evaluating this paper.

References

Baggaley, W. J. (2002), Radar observations, in *Meteors in the Earth's Atmosphere*, edited by E. Murad and I. P. Williams, pp. 123–148, Cambridge Univ. Press, Cambridge.

Dhomse, S. S., R. W. Saunders, W. Tian, M. P. Chipperfield, and J. M. C. Plane (2013), Plutonium-238 observations as a test of modeled transport and surface deposition of meteoric smoke particles, *Geophys. Res. Lett.*, *40*, 4454–4458, doi:10.1002/grl.50840.

Feng, W., D. R. Marsh, M. P. Chipperfield, D. Janches, J. Höffner, F. Yi, and J. M. C. Plane (2013), A global atmospheric model of meteoric iron, *J. Geophys. Res. Atmos.*, *118*, 9456–9474, doi:10.1002/jgrd.50708.

Fentzke, J. T., and D. Janches (2008), A semi-empirical model of the contribution from sporadic meteoroid sources on the meteor input function in the MLT observed at Arecibo, *J. Geophys. Res.*, *113*, A03304, doi:10.1029/2007JA012531.

Gardner, C. S., and A. Z. Liu (2007), Seasonal variations of the vertical fluxes of heat and horizontal momentum in the mesopause region at Starfire Optical Range, New Mexico, *J. Geophys. Res.*, *112*, D09113, doi:10.1029/2005JD006179.

Gardner, C. S., and A. Z. Liu (2010), Wave-induced transport of atmospheric constituents and its effect on the mesospheric Na layer, *J. Geophys. Res.*, *115*, D20302, doi:10.1029/2010JD014140.

Gardner, C. S., A. Z. Liu, D. R. Marsh, W. Feng, and J. M. C. Plane (2014), Inferring the global cosmic dust influx to the Earth's atmosphere from lidar observations of the vertical flux of mesospheric Na, *J. Geophys. Res. Space Physics*, *119*, 7870–7879, doi:10.1002/2014JA020383.

Huang, W., X. Chu, C. S. Gardner, Z. Wang, W. Fong, J. A. Smith, and B. R. Roberts (2013), Simultaneous, common-volume lidar observations and theoretical studies of correlations among Fe/Na layers and temperatures in the mesosphere and lower thermosphere at Boulder Table Mountain (40°N, 105°W), Colorado, *J. Geophys. Res. Atmos.*, *118*, 8748–8759, doi:10.1002/jgrd.50670.

Janches, D., C. J. Heinselman, J. L. Chau, A. Chandran, and R. Woodman (2006), Modeling the global micrometeor input function in the upper atmosphere observed by high power and large aperture radars, *J. Geophys. Res.*, *111*, A07317, doi:10.1029/2006JA011628.

Janches, D., S. Close, and J. T. Fentzke (2008), A comparison of detection sensitivity between ALTAIR and Arecibo meteor observations: Can high power and large aperture radars detect low velocity meteor head-echoes, *Icarus*, *193*(1), 105–111, doi:10.1016/j.icarus.2007.08.022.

Janches, D., L. P. Dyrud, S. L. Broadley, and J. M. C. Plane (2009), First observation of micrometeoroid differential ablation in the atmosphere, *Geophys. Res. Lett.*, *36*, L06101, doi:10.1029/2009GL037389.

Janches, D., J. M. C. Plane, D. Nesvorný, W. Feng, D. Vokrouhlický, and M. J. Nichols (2014), Radar detectability studies of slow and small Zodiacal Dust Cloud particles: I. The case of Arecibo 430 MHz meteor head echo observations, *Astrophys. J.*, *796*(41), 20, doi:10.1088/0004-637X/796/1/41.

Jessberger, E. K., T. Stephean, D. Rost, P. Arndt, M. Maetz, F. J. Stadermann, D. E. Brownlee, J. P. Bradley, and G. Kurat (2001), Properties of interplanetary dust: Information from collected samples, in *Interplanetary Dust*, vol I, edited by E. Grün et al., pp. 253–294, Springer, Berlin, Heidelberg, New York.

Langowski, M., C. von Savigny, J. P. Burrows, W. Feng, J. M. C. Plane, D. R. Marsh, D. Janches, M. Sinnhuber, and A. C. Aikin (2014), Global investigation of the Mg atom and ion layers using SCIAMACHY/Envisat observations between 70 km and 150 km altitude and WACCM-Mg model results, *Atmos. Chem. Phys. Discuss.*, *14*, 1971–2019, doi:10.5194/acpd-14-1971-2014.

Lodders, K., H. Palme, and H. P. Gail (2009), Abundances of elements in the solar system, in *Landolt Berstein New Series*, vol. VI/4B, edited by J. E. Trüper, chap. 4.4, pp. 560–630, Springer, Berlin, Heidelberg, New York.

Love, S. G., and D. E. Brownlee (1993), A direct measurement of the terrestrial mass accretion rate of cosmic dust, *Science*, *262*, 550.

Marsh, D. R., D. Janches, W. Feng, and J. M. C. Plane (2013a), A global model of meteoric sodium, *J. Geophys. Res. Atmos.*, *118*, 11,442–11,452, doi:10.1002/jgrd.50870.

Marsh, D. R., M. Mills, D. Kinnison, J.-F. Lamarque, N. Calvo, and L. Polvani (2013b), Climate change from 1850 to 2005 simulated in CESM1 (WACCM), *J. Clim.*, *26*(19), 7372–7391, doi:10.1175/JCLI-D-12-00558.1.

Mathews, J. D., D. Janches, D. D. Meisel, and Q. H. Zhou (2001), The micrometeoroid mass flux into the upper atmosphere: Arecibo results and a comparison with prior estimates, *Geophys. Res. Lett.*, *28*, 1929–1932, doi:10.1029/2000GL012621.

McBride, N., S. F. Green, and J. A. M. McDonnell (1999), Meteoroids and small sized debris in low Earth orbit and at 1 AU: Results of recent modeling, *Adv. Space Res.*, *23*, 73–82.

Nesvorný, D., P. Jenniskens, H. F. Levison, W. F. Bottke, D. Vokrouhlický, and M. Gounelle (2010), Cometary origin of the zodiacal cloud and carbonaceous micrometeorites. Implications for hot debris disks, *Astrophys. J.*, *713*, 816–836, doi:10.1088/0004-637X/713/2/816.

Nesvorný, D., D. Janches, D. Vokrouhlický, P. Pokorný, W. F. Bottke, and P. Jenniskens (2011), Dynamical model for the zodiacal cloud and sporadic meteors, *Astrophys. J.*, *743*, 129, doi:10.1088/0004-637X/743/2/129.

Pifko, S., D. Janches, S. Close, J. J. Sparks, T. Nakamura, and D. Nesvorný (2013), The meteoroid input function and predictions of mid-latitude meteor observations by the MU radar, *Icarus*, *223*, 444–459, doi:10.1016/j.icarus.2012.12.014.

Plane, J. M. C. (2004), A time-resolved model of the mesospheric Na layer: Constraints on the meteor input function, *Atmos. Chem. Phys.*, *4*(3), 627–638, doi:10.5194/acp-4-627-2004.

Plane, J. M. C. (2012), Cosmic dust in the Earth's atmosphere, *Chem. Soc. Rev.*, *41*(19), 6507–6518, doi:10.1039/C2CS35132C.

Vondrak, T., J. M. C. Plane, S. Broadley, and D. Janches (2008), A chemical model of meteoric ablation, *Atmos. Chem. Phys.*, *8*(23), 7015–7031, doi:10.5194/acp-8-7015-2008.